Gated adatoms on graphene studied with first-principles calculations

Kevin T. Chan, Hoonkyung Lee, and Marvin L. Cohen

Phys. Rev. B **83**, 035405 — Published 14 January 2011

DOI: 10.1103/PhysRevB.83.035405

Gated adatoms on graphene studied with first-principles calculations

Kevin T. Chan, Hoonkyung Lee, and Marvin L. Cohen
Department of Physics, University of California, Berkeley, California 94720 and
Materials Sciences Division, Lawrence Berkeley National Laboratory, Berkeley, California 94720
(Dated: December 13, 2010)

A first-principles pseudopotential density functional method for studying the gating of adatoms on graphene is presented. A variation in gate voltage is assumed to vary the number of electrons in the adatom-graphene system. The method is applied to the cases of Li and Co on graphene. The projected density of states, charge density, and local electrostatic potential are computed as a function of gate voltage. In the case of Li, the calculations show that the Li adatom can be ionized by changing the gate voltage, and that the ionization is accompanied by a sharp change in the electrotstatic potential of the adatom. In the case of Co, correlation in the 3*d* shell is treated using the LDA+U method, with several values of the U parameter considered. For $U = 2$ eV or greater, an ionization effect analogous to the case of Li is found for the Co adatom. This result is consistent with recent scanning tunneling spectroscopy experiments for Co on graphene.

PACS numbers: 73.22.Pr, 73.20.Hb, 73.20.At, 31.15.A-

I. INTRODUCTION

Graphene, a two-dimensional (2D) honeycomb lattice of carbon atoms, has been studied intensely in the past several years.[1,2] By now, many of its remarkable properties, such as its zero gap semiconducting electronic structure, massless Dirac quasiparticles, and anomalous Quantum Hall effects[3,4], are well known. The modification of pristine graphene is crucial for the study and elucidation of its properties, as well as for tailoring it for practical applications. Modifications that have received attention recently include growing or placing graphene on a variety of substrates,[5–9] applying mechanical strain,[10,11] patterning graphene into nanoribbons or dots,[12–14] and forming bi- or multi-layer graphene.[15,16]

Two important modifications are the variation of the carrier concentration of graphene via an applied gate voltage and the adsorption of adatoms or molecules on the graphene surface. It has been shown that gate voltages applied to graphene on a SiO_2 substrate can induce both electron and hole carriers up to a concentration of $n \sim 10^{13}$ cm^{-2} via the field effect.[17] With electrochemical gating, carrier concentrations of $n \gtrsim 10^{14}$ have been reported for graphene.[18,19] The field effect is possible because of the semimetallic nature of graphene, with linear DOS that vanishes at the charge neutrality point (NP) or Dirac point, and the 2D nature of graphene makes for a straightforward experimental geometry. The field effect was important in early measurements on graphene confirming high mobility and Dirac quasiparticles in graphene.[3–5,17]

As a 2D material, graphene is naturally amenable to the addition of adsorbates. Experimentally, adsorbates on graphene have been used as dopants that change the number of charge carriers,[20–22] as sources of scattering in transport measurements,[23] or as a method of band gap opening or otherwise altering the electronic structure of graphene.[16,24,25] In addition to considering the above phenomena, theoretical work on adsorbates on graphene has explored other possibilities, such as the formation of regular arrays of adsorbates, the existence of local moments, Kondo physics, and magnetically ordered arrays, and exotic phenomena such as atomic collapse.[26]

In graphene, variation of the gate voltage and adatom or molecule adsorption can be combined in the same system. In this way, the chemical potential of the adsorbate-graphene system can be precisely controlled. In some cases, such control can be used to explore the electronic structure of an adatom-graphene system over a range of energies;[23] in other cases, it can be used to carefully tune the properties of the adsorbate-graphene system, such as in the optimization of a graphene chemical sensor[22] or in the possible tuning of the Kondo effect.[27,28]

A recent scanning tunneling spectroscopy (STS) experiment demonstrated the ability to controllably ionize a Co adatom on graphene using either a back gate voltage or the STS tip bias voltage.[29] The charging of a localized state on a surface has been demonstrated using STS on other systems,[30–33] but those experiments lacked the precise control of ionization via backgate voltage that is possible on graphene. Given that STS is a natural tool for studying single adatoms on graphene, the amount of experimental data for STS on such systems should grow in the near future.

The unique opportunity that graphene presents to control the chemical potential of adsorbates on graphene using a gate voltage motivates the theoretical study of the gating of adatoms on graphene. In this work, we present a first-principles method for studying gated adatom-graphene systems. The method is applied to a prototype system, a Li adatom on graphene, as well as a more experimentally relevant case, Co on graphene. The electronic structure, including the density of states, charge density, and local electrostatic potential, is computed as a function of gate voltage. For both Li and Co on graphene, we find the presence of atomic-like states that remain localized on the

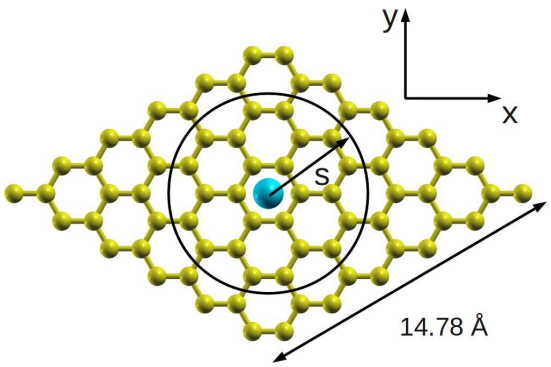

FIG. 1: (Color online) Adatom on hollow site in 6×6 unit cell. The view is along the $-z$ direction, perpendicular to the graphene plane. A circle of radius s centered around the adatom in the x-y plane is indicated.

adatom. Our results show that such states can be ionized by variation of the gate voltage, and that such ionization induces a sharp change in the local electrostatic potential, in agreement with the recent STS experiment. This method has the potential to be applied to a wide variety of other adatoms and molecular adsorbates.

The paper is organized as follows. In section II we present the model and details of the calculation. Sections III and IV present the results for Li and Co adatoms on graphene, respectively. In section V we discuss our results in relation to experiment, as well as some implications of our results. Section VI concludes the paper.

II. METHOD

A. Computational Framework

Our calculations are performed using the first-principles plane-wave pseudopotential method[34] and density-functional theory (DFT)[35,36] using the spin-polarized generalized gradient approximation functional of Perdew, Burke, and Ernzerhof (PBE).[37] The Quantum-ESPRESSO package[38] is used to perform the calculations. Ion cores are modeled using ultrasoft pseudopotentials.[3964] For C and Li, the $n = 1$ shell is treated as core and $n = 2$ as valence; for Co, $3s$ and $3p$ electrons are treated as core, while $4s$ and $3d$ are treated as valence. A nonlinear core correction is included for Li.[40] The electronic valence states are modeled using plane-waves with an energy cutoff of 45 Ry for the wavefunctions and 180 Ry for the charge density for Co on graphene, and 30 Ry and 120 Ry respectively for Li.

In the case of Co, we consider the possible strong correlations in the $3d$ shell using the so called LDA+U method[41] (or GGA+U in this work). In this approach, a Hubbard U term is added to the functional to model the Coulomb repulsion between $3d$ electrons localized on the Co atom. We use the rotationally-invariant formulation within a plane-wave psuedopotential framework, as described in Ref. 42. Note that a single Coulomb parameter U is used (the exchange parameter $J = 0$ eV). We consider three values for U: 0, 2 and 4 eV.

The calculations are performed for an adatom on graphene in a supercell with periodic boundary conditions. For the graphene in-plane (x-y) directions, a 6×6 supercell containing 72 C atoms and 1 adatom is used (Fig. 1). We use the lattice constant of 2.463 Å that we calculated for clean graphene; thus the distance between adatoms in our supercell arrangement is 14.78 Å. In the out-of-plane z direction perpendicular to the graphene plane, the unit cell length is 15 Å. The Brillouin zone is sampled using a $3 \times 3 \times 1$ Γ-centered k-point grid, and a Gaussian smearing of 0.05 eV is used for the electronic occupations.

The electronic density of states (DOS) is computed using a $21 \times 21 \times 1$ Γ-centered k-point grid (a 0.1 eV Gaussian smearing is used in the plots). The projected DOS (PDOS) is computed by projecting the electronic wavefunctions onto orthogonalized pseudoatomic orbitals; orbital occupations are obtained from the Löwdin analysis.

We consider three adsorption sites of high symmetry (as in Ref. 43): hollow (H), at the center of a hexagon; bridge (B), at the midpoint of a C-C bond; and top (T), on top of a C atom. The adsorption height h of the adatom, defined as the perpendicular distance between the adatom and the graphene plane (Fig. 2), is optimized such that the force on the adatom is less than 0.001 Ry/a.u. The C atoms in graphene are kept fixed at their coordinates for a perfect graphene sheet. For calculations of the same adatom at different levels of doping (discusssed in Section II B), the adatom height is optimized at zero doping (neutral charge) and then kept constant across all doping values. The effects of the approximation of fixed adatom height and C positions are discussed in Section V.

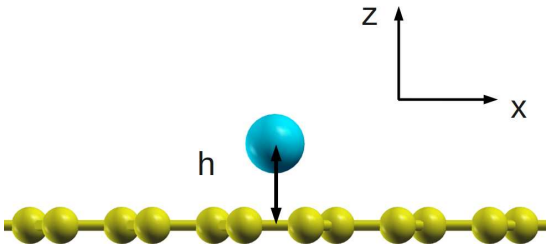

FIG. 2: (Color online) View of an adatom on graphene along the $+y$ direction of the unit cell. The height h is defined as the perpendicular distance above the graphene plane.

B. Modeling of the applied gate voltage

In experimental studies, the application of a gate voltage to the adatom-graphene system changes the total charge of the sample by adding or removing electrons and changing the chemical potential. We model this effect in our calculation by varying the total charge of the system from the neutral value by adding or removing electrons (doping the system). We consider several values of the total charge that range below and above neutral. For each given value of total charge considered, we fix the corresponding number of electrons per unit cell and perform a full self-consistent calculation of the electronic structure. Thus the Kohn-Sham electronic orbitals are allowed to relax according to the doping level. This method can be contrasted with a rigid-band model in which addition or removal of electrons changes the occupation of the electronic orbitals, but the orbitals themselves remain unchanged.

For a doping level away from neutral, the calculation involves a charged supercell. We employ a standard method for cancelling the divergence of the total energy for charged supercells, which is to add a compensating uniform (constant in space) background charge of opposite sign and with total magnitude equal to the net charge of the electrons plus ions in the system. (See, for example, Ref. 44.)

C. Supercell interactions

We briefly discuss the supercell interacations present in our calculations. In the z-direction perpendicular to the plane, the 15 Å separating periodic images is sufficient to make overlap of wavefunctions on neighboring images negligible. However, monopole (for charged systems), dipole, and higher order electrostatic interactions between periodic images are present. It is possible to correct for such interactions;[45,46] such corrections are not included in this work but are left for future study.

For the graphene in-plane directions, we take the 6×6 supercell containing one adatom and 72 C atoms to approximate a single adatom on an infinite graphene sheet. The choice of supercell size minimizes the bandwidth of localized atom-derived states while maintaining a reasonable computational cost. Due to their long range nature, electrostatic interactions between periodic images are not negligible. Therefore, we do not expect the long-range effects of gating adatoms on graphene to be captured accurately by our calculations. Note also that in order to model effects such as ionization of the adatom, one must dope the system on the order of 1 electron (e) per adatom, which corresponds to a charge density of 1 e/72 C, while in experiments for graphene on SiO_2, the doping range is approximately $\pm$ 1 e/1000 C. Despite the presence of long range electrostatic interactions between periodic images and the discrepancy with experimental doping level, we believe the 6×6 supercell is a reasonable approximation for the local behavior (within several Å) of the adatom on graphene under applied gate voltage.

Alternatively, for a system consisting of an adatom layer at a concentration of $\sim$ 1 adatom/72 C (as opposed to a single adatom) on graphene, the supercell interactions are physical and the 6×6 supercell is a reasonable approximation. However, in this case the large doping of $\sim 1e$/72 C may not be experimentally achievable.

III. LITHIUM ADATOM ON GRAPHENE

We consider the adsorption and gating of Li adatoms on graphene as a prototype. Li and other alkali atoms are often used in carbon nanotube and graphitic systems as a dopant, for example in graphite intercalation compounds.[47] Possessing one valence electron, an alkali adatom binds to graphene at the hollow site, transferring close to one electron to the graphene sheet, according to theoretical calculations.[43] In the present calculation, the Li atom is modeled with a pseudopotential with one valence electron in the $2s$ state.

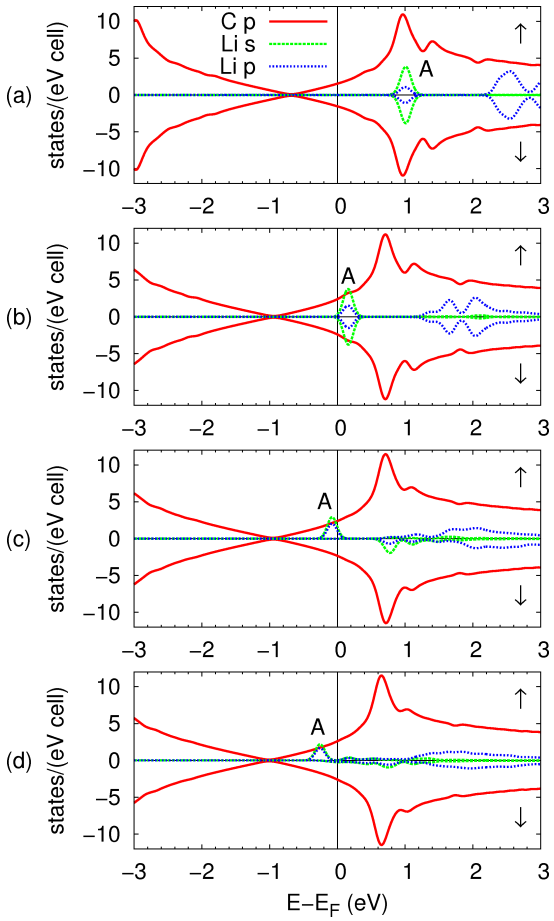

FIG. 3: (Color online) PDOS for Li adatom on graphene for various dopings: (a) 0 e (b) +1 e (c) +2 e (d) +3 e. Projections onto C $2p$ (solid red), Li $2s$ (dashed green), and Li $2p$ (dotted blue) are shown. Arrows indicate majority (up) and minority (down) spin channels. A state localized on the Li adatom is labeled A. Energies are relative to the Fermi energy E_F.

We reconfirm that the lowest energy binding site for Li on graphene is the hollow site. Our calculated adsorption height of 1.89 Å is somewhat larger than previous DFT-PBE calculations that treat Li $1s$ semicore states as valence[43,48,49] but is in good agreement with calculations for which Li $1s$ semicore states are treated as core.[50] Figure 3a shows the PDOS for the neutral Li-graphene system. The spin-up and spin-down states are degenerate. There is an atomic-like state A deriving from the Li $2s$ and $2p$ orbitals 1 eV above the Fermi level (E_F), while the Dirac point of the graphene DOS lies 0.7 eV below E_F. We interpret this result as a complete transfer of the single valence electron of the Li atom to the graphene sheet.

In Fig. 3, the PDOS for several levels of doping are plotted. The primary feature that we focus on is the ionization of the Li adatom as the doping is changed from 0 e to +3 e, or vice versa (unless otherwise noted, doping levels are quoted in number of electrons per unit cell, relative to neutral). Let us consider the progression from 0 e to +3 e doping. At a doping of +1 e, as in the 0 e case, a localized state A deriving from the Li atom is clearly distinguishable and remains unoccupied. At +2 e doping, the A state becomes partially occupied in the spin-up (majority) channel. Note also the splitting between up and down spins for the localized state, which is the same in origin as the splitting between occupied spin-up and unoccupied spin-down $2s$ states in an isolated Li atom. At +3 e doping, the Li spin-up peak A is completely occupied, with the Li spin-down states remaining unoccupied. We interpret this result as the increase in ionization state of the Li adatom by 1 e. Importantly, the A peak does not appear to hybridize with the graphene states at any level of doping, which suggests that the state is localized on the Li atom. Therefore, orbitals for the Li-graphene system can be assigned relatively unambigously to either the graphene or to the Li adatom.

When a free atom is ionized, the electrostatic potential due to the atom changes, since the contribution to screening of the potential from the added or removed electron changes. We find a similar effect for the ionization of the Li adatom on graphene. From our scf calculations, we extract the local electrostatic potential (bare ionic pseudopotential plus electronic Hartree potential), $V_{BH}(\vec{r})$, for the system. (In this work, "potential" refers to the potential energy

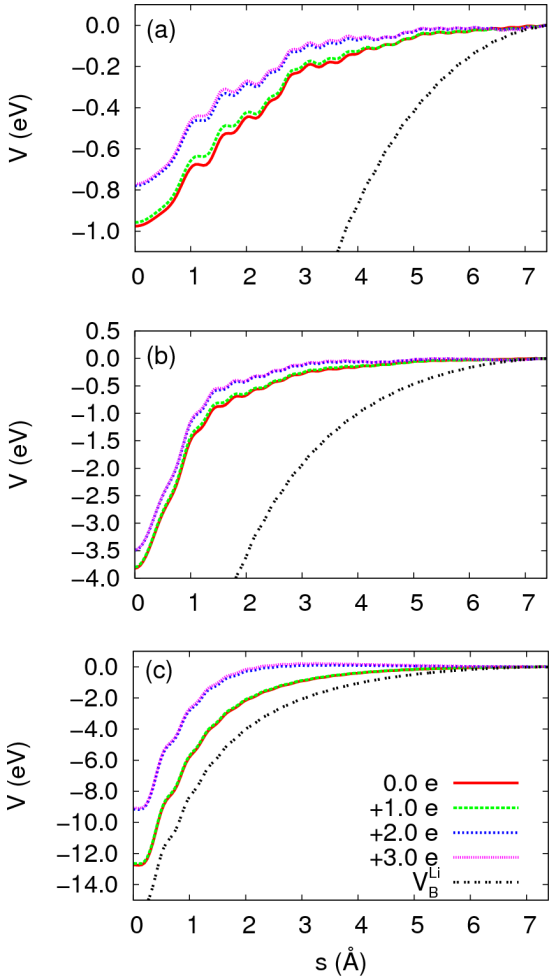

FIG. 4: (Color online) Plots of $\Delta V_{BH}(s,z)$ for a Li adatom on graphene for several doping values and at heights z = (a) 0 Å, (b) 0.7 Å, and (c) 2.7 Å above the graphene plane. The local ionic potential for Li, $V_B^{\rm Li}(s,z)$, is also plotted.

for an electron.) To compare V_{BH} for several different dopings, we consider the difference

$$\Delta V_{BH}(\vec{r}) = V_{BH}^{n}(\vec{r}) - V_{BH}^{\rm gr}(\vec{r}), \tag{1}$$

where V_{BH}^{n} is the potential for the adatom-graphene system with doping level n, and $V_{BH}^{\rm gr}$ is the potential for a clean graphene sheet with zero doping.

We consider the quantity

$$\Delta V_{BH}(s,z) = \frac{1}{2\pi s}\int_0^{2\pi} \Delta V_{BH}(s,\theta,z)d\theta, \tag{2}$$

the average of ΔV_{BH} over a a ring of radius s, centered around the adatom x-y position, at a height z above the graphene plane, and parallel to the plane (see Figs. 1 and 2); the position $\vec{r} = (s,\theta,z)$ is expressed in cylindrical coordinates. In Fig. 4 we plot $\Delta V_{BH}(s,z)$ for several different heights. The plots are aligned so that the potentials are zero at a distance from the adatom of $s = 7.39$ Å, equal to one-half the lattice constant of the 6×6 unit cell.[65] For comparison, we also plot $V_B^{\rm Li}(s,z)$, the local bare ionic pseudopotential for Li.

Compared with the potential at zero doping, the potential with $+1$ e has almost the same shape for all the heights plotted. However, the addition of another electron brings about a sharp change in the V_{BH}; the potential becomes significantly shallower. The addition of a further 1 e does not change the potential signifcantly, aside from a constant.

Comparing the potentials at different heights, we see that near the graphene sheet ($h = 0.0$ and 0.7 Å), the adatom potential is already screened strongly by the graphene electrons at 0 e doping, resulting in a V_{BH} that is much shallower than the bare ionic Li potential. The change in potential at $s = 0$ from $+1$ e to $+2$ e is about 0.3 eV. In

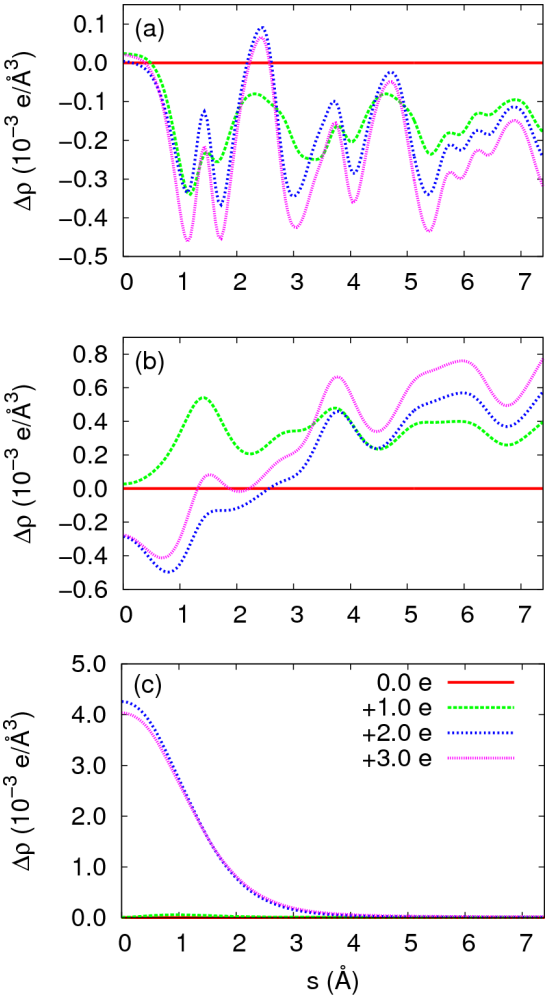

FIG. 5: (Color online) Plots of $\Delta\rho(s,z)$ for a Li adatom on graphene for several doping values and at heights z = (a) 0 Å, (b) 0.7 Å, and (c) 2.7 Å above the graphene plane.

contrast, the potential at $h = 2.7$ Å is weakly screened up to $+1$ e doping but becomes more strongly screened at $+2$ e doping, with a change in V_{BH} of approximately 4 eV at $s = 0$.

Comparison of the plots of the potential to the PDOS plots shows that filling of graphene-like states when going from 0 e to 1 e doping does not change the potential significantly (except by a constant), while the ionization of the Li adatom when increasing the doping from $+1$ e to $+2$ e corresponds to a sharp change in the shape of the potential. These changes in the potential can be understood by considering how the charge density changes as the doping level is increased. Define the charge density difference

$$\Delta\rho(\vec{r}) = \rho_n(\vec{r}) - \rho_0(\vec{r}), \tag{3}$$

where $\rho_n(\vec{r})$ is the charge density of the adatom-graphene system with doping level n, and $\rho_0(\vec{r})$ is the charge density at a reference doping level. For Li we take 0 e as the reference doping level. As we did for ΔV_{BH}, we take the circular average

$$\Delta\rho(s,z) = \frac{1}{2\pi s}\int_0^{2\pi} \Delta\rho(s,\theta,z)d\theta \tag{4}$$

for radius s and height z.

Figure 5 shows $\Delta\rho(s,z)$ for various heights. Upon filling the graphene-like states when going from 0 e to $+1$ e doping, the charge density near the graphene changes fairly uniformly across the 2D graphene plane, increasing at h = 0.7 Å and decreasing slightly at $h = 0$ Å. At $h = 2.7$ Å the charge density changes little. This result is consistent with the additional electrons occupying graphene π^* orbitals which lie above and below the graphene plane and are

delocalized across the graphene sheet. The local Hartree potential due to such a uniform (in the x-y plane) charge density is also uniform. Therefore the difference in V_{BH} between 0 e and +1 e should be nearly constant, as is found in our calculations.

On the other hand, when the doping is increased from +1 e to +2 e, the charge density at $h = 2.7$ Å shows a much larger increase near the adatom than away from it, while nearer to the graphene plane, the charge density change is small. (At $h = 0.7$ Å the charge density actually decreases near the adatom and increases away from it, but the magnitude of charge density change is small compared with that calculated at $h = 2.7$ Å.) This charge density change corresponds to occupation of an orbital localized on the Li adatom, above the graphene plane (i.e., ionization of the Li adatom). Since the local Hartree potential is greater at points of greater charge density, the large increase in charge density near the Li adatom increases V_{BH} near the adatom relative to points further from the adatom, consistent with our calculations. Furthermore, the change in V_{BH} is sharp because the charge density is concentrated on the adatom, rather than spread out over a plane.

A notable feature of the PDOS is the change in orbital character of the A peak. At 0 e doping, the A peak has mostly Li 2s character, but has some 2p character, since the spherical symmetry of the potential near the Li adatom is broken by the graphene. As the doping is increased, the 2s character of the peak decreases and the 2p character increases. A possible explanation is that the orbital becomes more extended into the vacuum and less localized on the Li adatom. The orbital becomes more extended because the increase in charge on the graphene increases the Hartree potential, pushing the wavefunction away from the graphene.

To summarize the results for Li on graphene, the PDOS calculations show that the Li adatom is ionized when the doping is increased or decreased between 0 e and +3 e. The ionization corresponds to a large change in charge density localized on the Li adatom and a sharp change in V_{BH}, in analogy with the ionization of a free atom.

IV. COBALT ADATOM ON GRAPHENE

Our study of Co adatoms on graphene is motivated by recent STS experiments on this system, in which it was found that the Co adatom could be controllably ionized by gate or tip bias voltage.[29] In addition, the Co atom has a partially occupied 3d shell and therefore has the possibility of forming a local moment on graphene. Several theoretical works have studied the Kondo physics of Co on graphene[51–53] and of adatoms on graphene in general,[27,54–57] but we do not consider the Kondo effect in this work.

Following the example of Li on graphene presented in Section III, we start with the undoped case. For plain GGA ($U = 0$ eV) we find that the lowest energy binding site is the H site with a binding height of 1.56 Å above graphene, in reasonable agreement with other works.[51–53,58–60] For $U = 2$ and 4 eV, we also find the H site to be lowest in energy, with heights of 1.75 and 1.88 Å, respectively.[66]

Figures 6c, 7c, and 8c show the PDOS for the neutral Co-graphene system for the three values of U considered in this work. Due to symmetry, the five 3d orbitals (for a given spin) split into a singly degenerate A_1 orbital, deriving from the d_{z^2} atomic orbital, a doubly degenerate E_1 orbital, derving from d_{zx} and d_{zy} orbitals, and a doubly degenerate E_2 orbital, deriving from $d_{x^2-y^2}$ and d_{xy} orbitals. The E_1 and E_2 orbitals hybridize strongly with the graphene sheet, while the A_1 and 4s orbitals hybridize weakly or not at all with graphene, although they can hybridize with each other.

For $U = 0$ eV, the spin-up Co 3d states are almost completely occupied (occupancy 4.7), while the spin-down 3d states are partially occupied (occupancy 3.6), with the E_1 orbital lying at E_F. The spin-up and spin-down Co 4s states have occupancies close to zero (0.1). Thus the Co atom orbital occupation is $3d^{8.3}4s^{0.2}$. The Dirac point E_D of the graphene lies slightly below E_F, indicating a small amount of charge transfer from Co to graphene, consistent with the reduction in occupation on the Co atom from 9 for the free atom to 8.5 on graphene.

The addition of a U of 2 eV changes the PDOS significantly. In comparison to the $U = 0$ eV case, the 3d levels are shifted away from E_F, and the occupations of the 3d levels are pushed to near-integer values. These effects are typical for the LDA+U method.[41] The spin-up 3d states remain near-fully occupied (occupancy 4.9), while the spin-down 3d state occupancy is 3.0; the E_1 orbitals have been pushed ∼1.0 eV above E_F by the addition of the U, and their occupation is reduced to zero. On the other hand, the spin-up Co 4s state is partially occupied (occupancy 0.7) and lies at E_F. In this case, the Co atom orbital occupation is $3d^{7.9}4s^{0.7}$. The effect of the additional $U = 2$ eV is to transfer approximately 0.5 e from the 3d orbital to the 4s orbital of Co.

The $U = 4$ eV case is similar to the $U = 2$ eV case. The Co 4s states and E_D have approximately the same position relative to E_F, and the occupancies of the Co 3d states are the same. However, the Co 3d states are shifted further from E_F by the larger U value.

Our PDOS calculations for $U = 0$ eV (plain GGA) are in good agreement with previous works.[53,59,60] In addition, our PDOS for $U = 0$ and $U = 2$ eV correspond well to two configurations found in another work (Figs. 1(a) and 1(b) in Ref. 52).

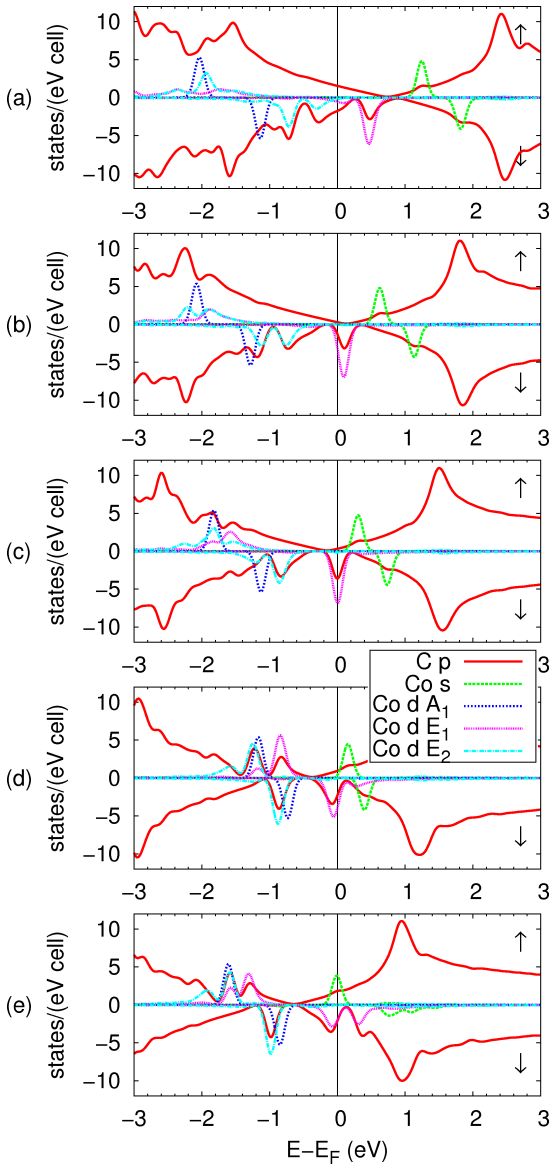

FIG. 6: (Color online) PDOS for Co adatom on graphene with $U = 0$ eV for various dopings: (a) -2 e (b) -1 e (c) 0 e (d) $+1$ e (e) $+2$ e. Projections onto C $2p$ (solid red), Co $4s$ (dashed green), Co $3d$ A_1 (dotted blue), Co $3d$ E_1 (small-dotted magenta), and Co $3d$ E_2 (dash-dotted cyan) are shown. Arrows indicate majority (up) and minority (down) spin channels. Energies are relative to the Fermi energy E_F.

We now consider the doping dependence of the PDOS for Co on graphene. Figure 6 shows the PDOS for $U = 0$ eV for various levels of doping. At a doping of -2 e, the spin-down E_1 orbital is unoccupied, as are some graphene π states, with E_D lying above E_F. As the doping is increased, the occupation of the spin-down E_1 orbital increases, as does the occupation of both spin-up and spin-down graphene states. We find that as the occupation of the spin-down E_1 orbital changes, the orbital stays pinned to E_F, in contrast to the graphene-derived states. Comparing the energy of the E_1 peak to the Dirac point of graphene, we find that at low doping, when E_1 is unoccupied, it lies below E_D, but at high doping, E_1 becomes mostly occupied and its energy is above E_D. The increase in occupation of the $3d$ shell coincides with a shift towards higher energy of the occupied $3d$ levels as well. Increasing the doping from $+1$ e to $+2$ e, The occupations of both the spin-down E_1 and spin-up $4s$ orbitals increase simultaneously.

The PDOS for U= 2 eV and $U = 4$ eV (Figs. 7 and 8) show similar trends with respect to gating that differ from the $U = 0$ eV case. We focus the discussion on the results for the $U = 2$ eV calculations. As for the case of Li, we focus on the ionization of the Co adatom by gating. Just as for the zero doping case, for doping levels between -2 e and $+2$ e, the effect of the U is to shift the $3d$ levels away from E_F. As a result, the effect of gating is to ionize the Co adatom by occupying or unoccupying the $4s$ level, which is localized on Co and hybridizes only weakly with

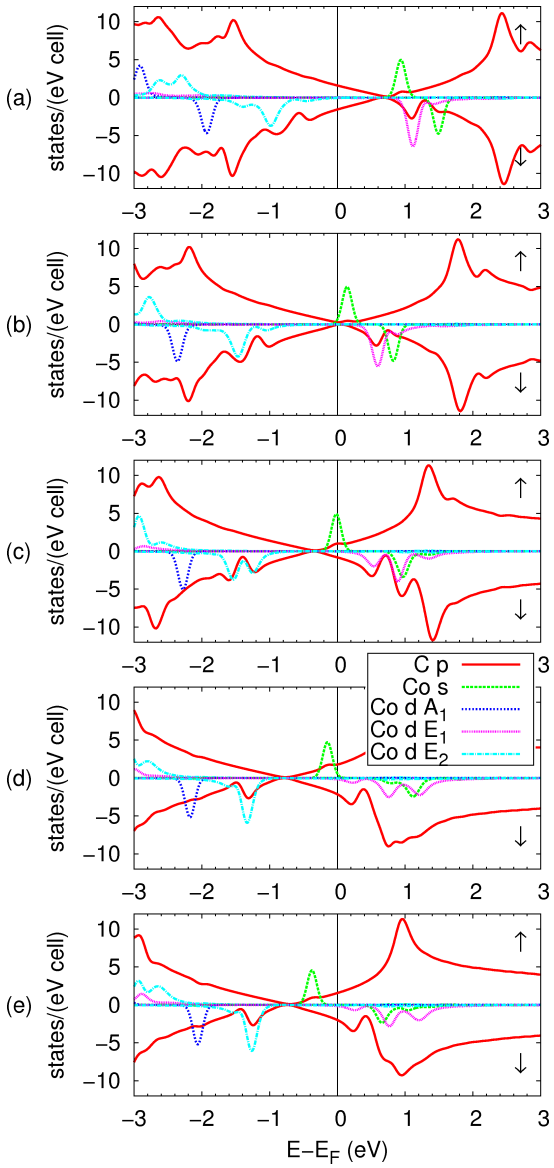

FIG. 7: (Color online) PDOS for Co adatom on graphene with $U = 2$ eV for various dopings: (a) -2 e (b) -1 e (c) 0 e (d) $+1$ e (e) $+2$ e. Projections onto C $2p$ (solid red), Co $4s$ (dashed green), Co $3d$ A_1 (dotted blue), Co $3d$ E_1 (small-dotted magenta), and Co $3d$ E_2 (dash-dotted cyan) are shown. Arrows indicate majority (up) and minority (down) spin channels. Energies are relative to the Fermi energy E_F.

graphene.

The ionization of Co by changing the occupation of the $4s$ level is analogous to the ionization of Li by changing the occupation of the $2s$ level. In Figs. 9 and 10, we plot $\Delta V_{BH}(s,z)$ and $\Delta\rho_{BH}(s,z)$ for Co on graphene with $U = 2$ eV at selected heights for several doping values. The quantities $\Delta V_{BH}(s,z)$ and $\Delta\rho_{BH}(s,z)$ are defined in Eqs. 1-4, in the same way as for Li. The bare ionic pseudopotential for Co, $V_B^{\rm Co}(s,z)$, is also plotted. Note that the Co ion core has charge $+9$ e, so that even at -2 e doping of the Co-graphene system, the ionic potential is screened by ~ 8 electrons localized on the Co adatom, unlike in the Li case. For Co, we take -2 e as the reference doping level for $\rho_0(\vec{r})$ in the definition of $\Delta\rho(\vec{r})$ (Eq. 3). Just as in the Li case, V_{BH} for the graphene case shows a sharp change upon ionization of the Co adatom, and the added charge density that ionizes Co is localized close to the adatom (within a few Å in the x-y plane). Furthermore, the change in the charge density near the graphene plane for Co (Figs. 10(a) and (b)) is simlar to the case of Li (Figs. 5(a) and (b)).

Interestingly, in the $U = 4$ eV case, when the doping changes from $+1$ e to $+2$ e, the configuration of the $3d$ shell changes abruptly. The A_1 state becomes unoccupied, while the E_1 state becomes occupied. Apparently, at a large enough doping, increasing the occupation of the $3d$ shell becomes favorable, but in order to satisfy near-integer

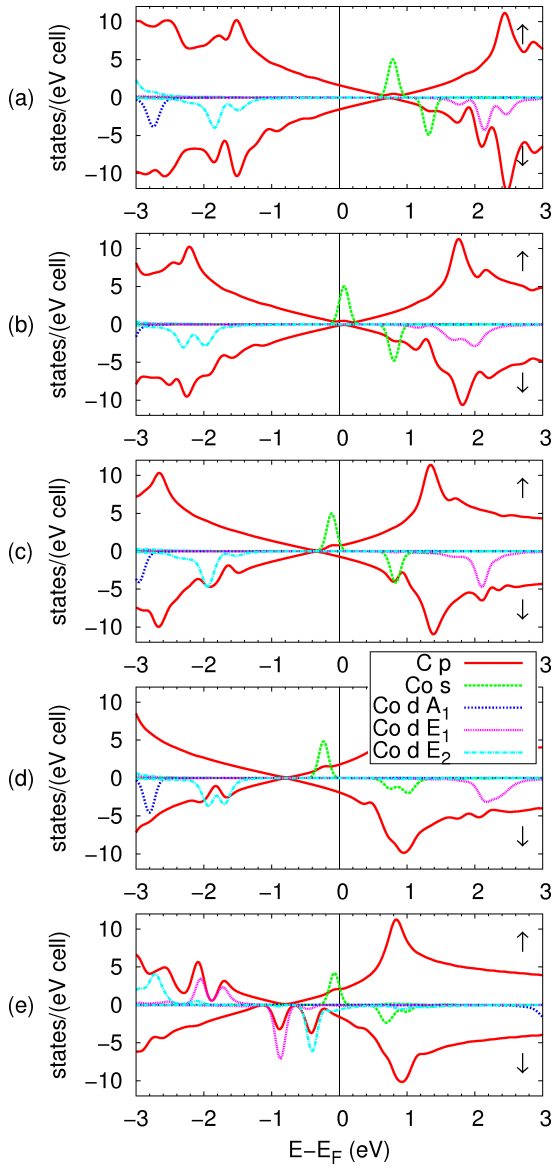

FIG. 8: (Color online) PDOS for Co adatom on graphene with $U = 4$ eV at various dopings: (a) -2 e (b) -1 e (c) 0 e (d) $+1$ e (e) $+2$ e. Projections onto C $2p$ (solid red), Co $4s$ (dashed green), Co $3d$ A_1 (dotted blue), Co $3d$ E_1 (small-dotted magenta), and Co $3d$ E_2 (dash-dotted cyan) are shown. Arrows indicate majority (up) and minority (down) spin channels. Energies are relative to the Fermi energy E_F.

occupations of the orbitals (favored by the LDA+U), the doubly degenerate E_1 orbital becomes (approximately) fully occupied, rather than occupying the A_1 orbital and partially occupying the E_1 orbital.

To summarize the results for Co on graphene, we find that the choice of the U parameter has significant effects on the PDOS. For $U = 0$ eV, the gate voltage can change the occupation of both $3d$ and $4s$ orbitals. For $U = 2$ or 4 eV, the gate voltage can ionize the $4s$ orbital in a manner analogous to the Li adatom case.

V. DISCUSSION

In this section, we discuss some implications of this work. In Ref. 29, Co atoms on a graphene surface with a controllable gate voltage were studied using scanning tunneling spectroscopy. Our calculations for Co on graphene are in agreement with the experimental results in several respects. In our calculations of the PDOS, we find resonances near E_F that derive from Co adatom states, and these resonances are localized around the adatom. Similarly, the experimentally measured differential conductance (dI/dV) on top of the Co atom shows resonances near E_F.

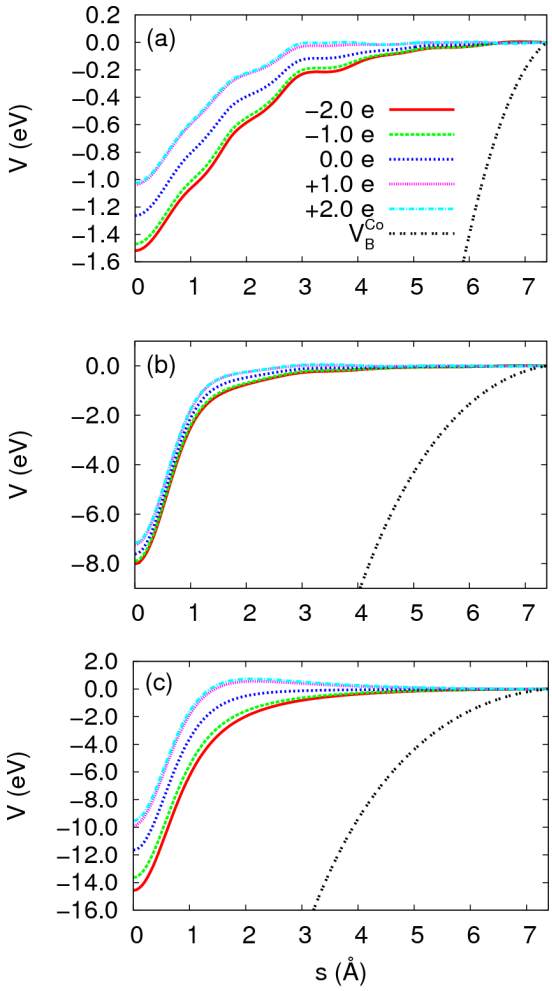

FIG. 9: (Color online) Plots of $\Delta V_{BH}(s,z)$ for a Co adatom on graphene with $U = 2$ eV for several doping values and at heights $z =$ (a) 0 Å, (b) 0.7 Å, and (c) 2.7 Å above the graphene plane. The local ionic potential for Co, $V_B^{\rm Co}(s,z)$, is also plotted.

Although experimentally these resonances cannot be identified unambiguously as coming from Co atomic-like states, their behavior with respect to a change in gate voltage was measured and is in agreement with the behavior of the peaks in our calculation. In both cases, the position of the resonances relative to E_F can be shifted by application of the gate voltage. In particular, the peaks can be shifted above or below E_F, changing the occupation of the atomic-like state and the ionization state of the adatom.

Furthermore, our calculation shows that the change in ionization of the Co adatom is accompanied by a sharp change in the electrostatic potential at and around the adatom. This sharp change in the potential is induced whenever the adatom is ionized, whether by the gate voltage or by the STS tip. The sharp change in the potential upon ionization is consistent with a large response in the dI/dV signal seen in experiment, both when varying the tip-sample bias with the STS tip above the adatom, and when varying the tip position at fixed gate and bias voltages.

In these respects, our calculation is in good qualitative agreement with several features in experiment. Due to several approximations in our calculation, the agreement with experiment cannot be considered quantitative, but by treating these approximations more exactly, the calculations might be brought in better quantitative agreement. In our calculation, we neglect the SiO_2 substrate upon which the graphene sits in experiment. It is known that graphene on SiO_2 has corrugations[61] and "charge puddles"[62] that can affect the electronic structure of graphene. However, the charge puddles cause fluctuations in E_D of only 30 meV and have spatial width of 20 nm, so on the scale of an atom, the charge puddles only shift the reference doping level for zero applied gate voltage. The corrugations could have some effect on the binding site and geometry of the Co adatom on graphene.

Our calculations also assume that the C and adatom positions remain fixed as the doping level is changed. In previous studies for a variety of adatoms on graphene, it was found that adatom adsorption on the H site induced little distortion in the graphene lattice.[43] Therefore, for the undoped adatom-graphene system, a rigid graphene

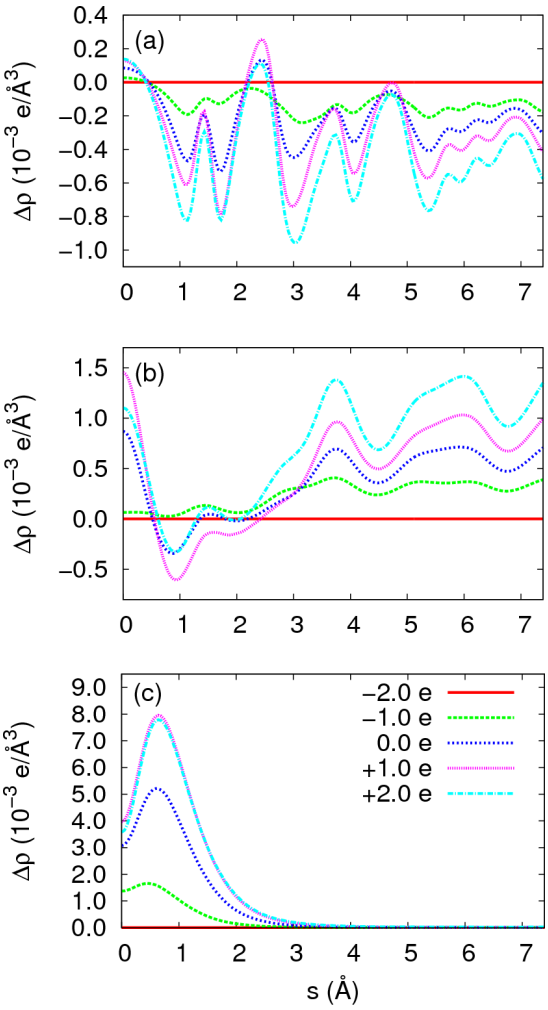

FIG. 10: (Color online) Plots of $\Delta\rho(s,z)$ for a Co adatom on graphene with $U = 2$ eV for several doping values and at heights $z =$ (a) 0 Å, (b) 0.7 Å, and (c) 2.7 Å above the graphene plane.

lattice approximation is reasonable. Upon doping, we might expect the adatom height to change somewhat. This could affect the hybridization between the adatom and graphene in the case of Co. We do not expect doping to distort the graphene lattice much because the change in charge density is mostly either delocalized across the graphene plane or, when localized, centered on the adatom, not on the C atoms. The exception might be Co for $U = 0$ eV, in which case some distortion and shifting of energy levels is possible.

Another approximation is the use of Kohn-Sham eigenvalues for the electronic spectra. While this approximation often gives reasonable results, the spectra may be modified by many-body effects. The use of three values for U in our calculations reflects some uncertainty in the treatment of correlation in the Co-graphene system. Our results show that the value of U affects the binding height and the character of the Co resonances near E_F in the electronic DOS. Other works in the literature have considered other approximations to correlation in this system,[51–53] and further work on this topic would be worthwhile.

The effects of the supercell approximation have been considered in Section II C. We also note that the experimental results include the effects of the STM tip, but our calculation does not include such effects.

Despite these approximations, our calculations capture well the experimental observation of gate-induced ionization, and there is the possibility of further quantitative improvement of these calculations.

In the case of Li on graphene, we found that the Li adatom can be controllably ionized by the gate voltage in a manner similar to the Co case. Such ionization may not be experimentally realizable due to the large energy difference between the Li atomic-like state and E_D. Nevertheless, Li on graphene serves as a model system to understand the gating of adatoms on graphene theoretically.

The gating of adatoms on graphene opens the possibility of controllably tuning the chemistry of adatoms or molecules on a graphene surface by the application of a gate voltage, which would have many exciting possibilites for catalysis,

hydrogen storage,[63] and other applications which may yet be discovered. The periodic table offers a wide variety of atoms for experimental and theoretical study, not to mention molecules. While not all atoms or molecules will be gateable experimentally, the method described in this work can be used to search for and predict specific adsorbates for which tuning the electronic structure by gating is experimentally realizable.

VI. CONCLUSION

In conclusion, this work presents a method for studying the gating of atoms on graphene using first principles calculations. A Li adatom on graphene serves as a useful model for understanding the gating of adatoms on graphene. By calculating the electronic structure, including the PDOS, potential, and charge density, we demonstrate the ionization of a Li adatom by doping and a concomitant sharp change in the electrostatic potential. Calculations for Co on graphene demonstrate an ionization effect, analogous to the Li case, which is in good agreement with experimental results. We discuss the various approximations used in this work, and consider ways to improve upon them. Using this method to study other adatoms or molecules may yield interesting new results that can be verified in experiment and may lead to practical applications.

Acknowledgments

We are grateful to Victor Brar and Regis Decker for useful discussions. This work was supported by National Science Foundation Grant No. DMR07-05941 and by the Director, Office of Science, Office of Basic Energy Sciences, Materials Sciences and Engineering Division, U.S. Department of Energy under Contract No. DE-AC02-05CH11231. Computational resources have been provided by DOE at Lawrence Berkeley National Laboratory's NERSC facility and the Lawrencium computational cluster resource provided by the IT Division at the Lawrence Berkeley National Laboratory.

[1] A. K. Geim and K. S. Novoselov, Nat Mater **6**, 183 (2007).
[2] A. K. Geim, Science **324**, 1530 (2009).
[3] K. S. Novoselov, A. K. Geim, S. V. Morozov, D. Jiang, M. I. Katsnelson, I. V. Grigorieva, S. V. Dubonos, and A. A. Firsov, Nature **438**, 197 (2005).
[4] Y. Zhang, Y.-W. Tan, H. L. Stormer, and P. Kim, Nature **438**, 201 (2005).
[5] K. S. Novoselov, D. Jiang, F. Schedin, T. J. Booth, V. V. Khotkevich, S. V. Morozov, and A. K. Geim, Proceedings of the National Academy of Sciences of the United States of America **102**, 10451 (2005).
[6] J. C. Meyer, A. K. Geim, M. I. Katsnelson, K. S. Novoselov, T. J. Booth, and S. Roth, Nature **446**, 60 (2007).
[7] C. Berger, Z. Song, T. Li, X. Li, A. Y. Ogbazghi, R. Feng, Z. Dai, A. N. Marchenkov, E. H. Conrad, P. N. First, et al., The Journal of Physical Chemistry B **108**, 19912 (2004).
[8] A. Reina, X. Jia, J. Ho, D. Nezich, H. Son, V. Bulovic, M. S. Dresselhaus, and J. Kong, Nano Letters **9**, 30 (2009).
[9] K. S. Kim, Y. Zhao, H. Jang, S. Y. Lee, J. M. Kim, K. S. Kim, J.-H. Ahn, P. Kim, J.-Y. Choi, and B. H. Hong, Nature **457**, 706 (2009).
[10] Z. H. Ni, T. Yu, Y. H. Lu, Y. Y. Wang, Y. P. Feng, and Z. X. Shen, ACS Nano **2**, 2301 (2008).
[11] T. M. G. Mohiuddin, A. Lombardo, R. R. Nair, A. Bonetti, G. Savini, R. Jalil, N. Bonini, D. M. Basko, C. Galiotis, N. Marzari, et al., Phys. Rev. B **79**, 205433 (2009).
[12] M. Y. Han, B. Özyilmaz, Y. Zhang, and P. Kim, Phys. Rev. Lett. **98**, 206805 (2007).
[13] X. Li, X. Wang, L. Zhang, S. Lee, and H. Dai, Science **319**, 1229 (2008).
[14] L. A. Ponomarenko, F. Schedin, M. I. Katsnelson, R. Yang, E. W. Hill, K. S. Novoselov, and A. K. Geim, Science **320**, 356 (2008).
[15] K. S. Novoselov, E. McCann, S. V. Morozov, V. I. Fal/'ko, M. I. Katsnelson, U. Zeitler, D. Jiang, F. Schedin, and A. K. Geim, Nat Phys **2**, 177 (2006).
[16] T. Ohta, A. Bostwick, T. Seyller, K. Horn, and E. Rotenberg, Science **313**, 951 (2006).
[17] K. S. Novoselov, A. K. Geim, S. V. Morozov, D. Jiang, Y. Zhang, S. V. Dubonos, I. V. Grigorieva, and A. A. Firsov, Science **306**, 666 (2004).
[18] A. Das, S. Pisana, B. Chakraborty, S. Piscanec, S. K., Saha, W. U.V., K. Novoselov, H. Krishnamurthy, A. Geim, A. Ferrari, et al., Nat Nano **3**, 210 (2008).
[19] D. K. Efetov and P. Kim, arXiv:1009.2988.
[20] A. Bostwick, T. Ohta, T. Seyller, K. Horn, and E. Rotenberg, Nat Phys **3**, 36 (2007).
[21] I. Gierz, C. Riedl, U. Starke, C. R. Ast, and K. Kern, Nano Letters **8**, 4603 (2008).
[22] F. Schedin, A. K. Geim, S. V. Morozov, E. W. Hill, P. Blake, M. I. Katsnelson, and K. S. Novoselov, Nat Mater **6**, 652 (2007).
[23] J.-H. Chen, C. Jang, S. Adam, M. S. Fuhrer, E. D. Williams, and M. Ishigami, Nat Phys **4**, 377 (2008).
[24] D. A. Dikin, S. Stankovich, E. J. Zimney, R. D. Piner, G. H. B. Dommett, G. Evmenenko, S. T. Nguyen, and R. S. Ruoff, Nature **448**, 457 (2007).
[25] D. C. Elias, R. R. Nair, T. M. G. Mohiuddin, S. V. Morozov, P. Blake, M. P. Halsall, A. C. Ferrari, D. W. Boukhvalov, M. I. Katsnelson, A. K. Geim, et al., Science **323**, 610 (2009).
[26] A. H. Castro Neto, F. Guinea, N. M. R. Peres, K. S. Novoselov, and A. K. Geim, Rev. Mod. Phys. **81**, 109 (2009).
[27] K. Sengupta and G. Baskaran, Phys. Rev. B **77**, 045417 (2008).
[28] J. Chen, W. G. Cullen, E. D. Williams, and M. S. Fuhrer, arXiv:1004.3373.
[29] V. W. Brar, R. Decker, H. Solowan, Y. Wang, L. Maserati, K. T. Chan, H. Lee, C. O. Girit, A. Zettl, S. G. Louie, et al., Nat Phys, to be published.
[30] N. A. Pradhan, N. Liu, C. Silien, and W. Ho, Phys. Rev. Lett. **94**, 076801 (2005).
[31] G. V. Nazin, X. H. Qiu, and W. Ho, Phys. Rev. Lett. **95**, 166103 (2005).
[32] F. Marczinowski, J. Wiebe, F. Meier, K. Hashimoto, and R. Wiesendanger, Phys. Rev. B **77**, 115318 (2008).
[33] K. Teichmann, M. Wenderoth, S. Loth, R. G. Ulbrich, J. K. Garleff, A. P. Wijnheijmer, and P. M. Koenraad, Phys. Rev. Lett. **101**, 076103 (2008).
[34] J. Ihm, A. Zunger, and M. L. Cohen, Journal of Physics C: Solid State Physics **12**, 4409 (1979).
[35] P. Hohenberg and W. Kohn, Phys. Rev. **136**, B864 (1964).
[36] W. Kohn and L. J. Sham, Phys. Rev. **140**, A1133 (1965).
[37] J. P. Perdew, K. Burke, and M. Ernzerhof, Phys. Rev. Lett. **77**, 3865 (1996).
[38] P. Giannozzi, S. Baroni, N. Bonini, M. Calandra, R. Car, C. Cavazzoni, D. Ceresoli, G. L. Chiarotti, M. Cococcioni, I. Dabo, et al., Journal of Physics: Condensed Matter **21**, 395502 (2009).
[39] D. Vanderbilt, Phys. Rev. B **41**, 7892 (1990).
[40] S. G. Louie, S. Froyen, and M. L. Cohen, Phys. Rev. B **26**, 1738 (1982).
[41] V. I. Anisimov, F. Aryasetiawan, and A. I. Lichtenstein, Journal of Physics: Condensed Matter **9**, 767 (1997).
[42] M. Cococcioni and S. de Gironcoli, Phys. Rev. B **71**, 035105 (2005).
[43] K. T. Chan, J. B. Neaton, and M. L. Cohen, Phys. Rev. B **77**, 235430 (2008).
[44] G. Makov and M. C. Payne, Phys. Rev. B **51**, 4014 (1995).
[45] L. Bengtsson, Phys. Rev. B **59**, 12301 (1999).
[46] P. Gava, M. Lazzeri, A. M. Saitta, and F. Mauri, Phys. Rev. B **79**, 165431 (2009).

[47] M. S. Dresselhaus and G. Dresselhaus, Advances in Physics **30**, 139 (1981).
[48] S. Meng and S. Gao, The Journal of Chemical Physics **125**, 014708 (pages 10) (2006).
[49] F. Valencia, A. H. Romero, F. Ancilotto, and P. L. Silvestrelli, The Journal of Physical Chemistry B **110**, 14832 (2006).
[50] K. Rytkönen, J. Akola, and M. Manninen, Phys. Rev. B **75**, 075401 (2007).
[51] T. O. Wehling, H. P. Dahal, A. I. Lichtenstein, M. I. Katsnelson, H. C. Manoharan, and A. V. Balatsky, Phys. Rev. B **81**, 085413 (2010).
[52] T. O. Wehling, A. V. Balatsky, M. I. Katsnelson, A. I. Lichtenstein, and A. Rosch, Phys. Rev. B **81**, 115427 (2010).
[53] D. Jacob and G. Kotliar, arXiv:1006.2779.
[54] K. Saha, I. Paul, and K. Sengupta, Phys. Rev. B **81**, 165446 (2010).
[55] B. Uchoa, L. Yang, S.-W. Tsai, N. M. R. Peres, and A. H. Castro Neto, Phys. Rev. Lett. **103**, 206804 (2009).
[56] H.-B. Zhuang, Q. feng Sun, and X. C. Xie, EPL (Europhysics Letters) **86**, 58004 (5pp) (2009).
[57] Z.-G. Zhu, K.-H. Ding, and J. Berakdar, EPL (Europhysics Letters) **90**, 67001 (2010).
[58] Y. Yagi, T. M. Briere, M. H. F. Sluiter, V. Kumar, A. A. Farajian, and Y. Kawazoe, Phys. Rev. B **69**, 075414 (2004).
[59] Y. Mao, J. Yuan, and J. Zhong, Journal of Physics: Condensed Matter **20**, 115209 (2008).
[60] C. Cao, M. Wu, J. Jiang, and H.-P. Cheng, Phys. Rev. B **81**, 205424 (2010).
[61] M. Ishigami, J. H. Chen, W. G. Cullen, M. S. Fuhrer, and E. D. Williams, Nano Letters **7**, 1643 (2007).
[62] Y. Zhang, V. W. Brar, C. Girit, A. Zettl, and M. F. Crommie, Nat Phys **5**, 722 (2009).
[63] H. Lee, W. I. Choi, and J. Ihm, Phys. Rev. Lett. **97**, 056104 (2006).
[64] We used the pseudopotentials C.pbe-rrkjus.UPF, Li.pbe-n-van.UPF, and Co.pbe-nd-rrkjus.UPF from http://www.quantum-espresso.org.
[65] A more natural way to align the potentials would be to set them to zero at a distance far from the adatom, where the potential is close to that of a clean graphene sheet, but due to the limited supercell size in the calculation, the potential at the edge of the unit cell is not converged to the clean graphene limit.
[66] If the C atoms in graphene are allowed to relax, the H site remains the lowest in energy for $U = 0$ and 2 eV, but the T site is lowest in energy for $U = 4$ eV. This result is consistent with Ref. 52.

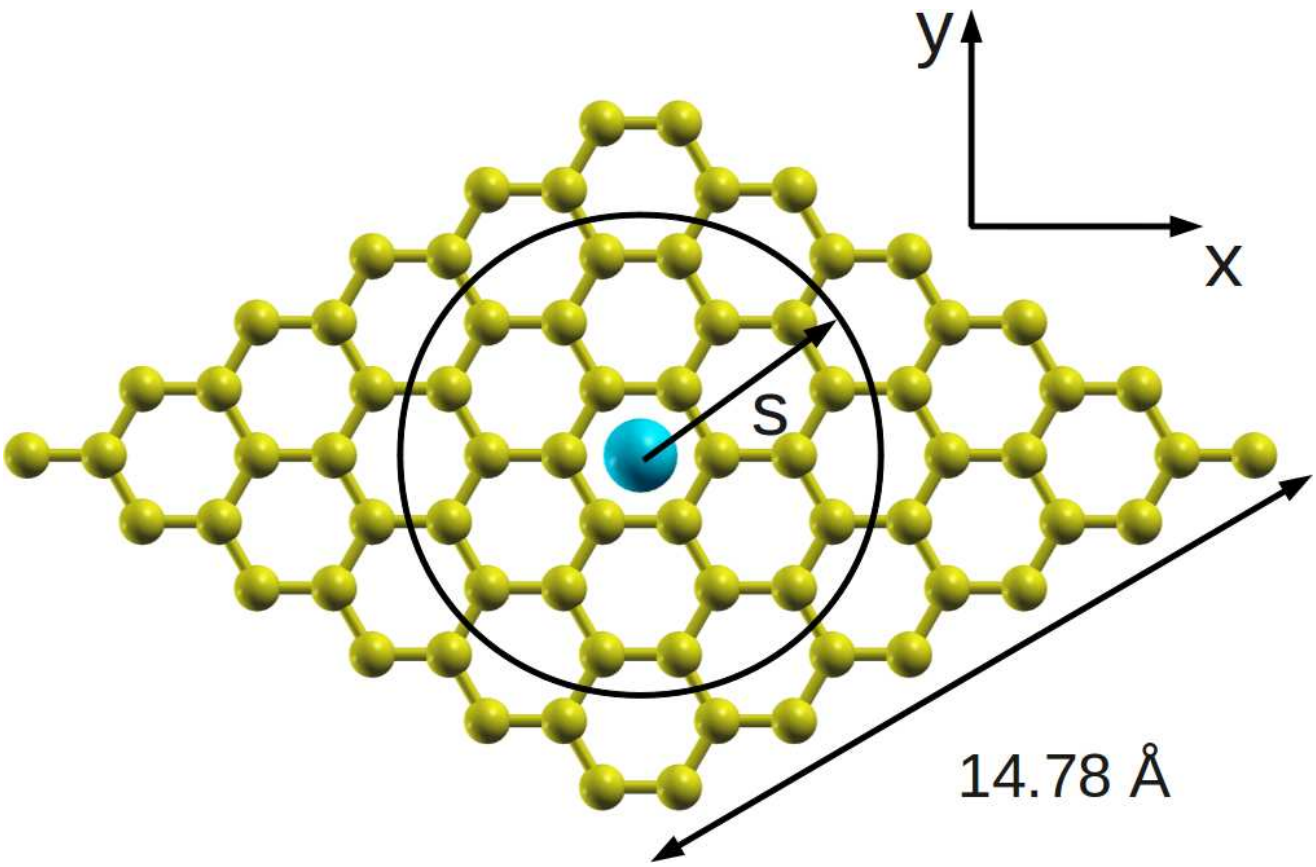

Figure 1 BX11058 13Dec2010

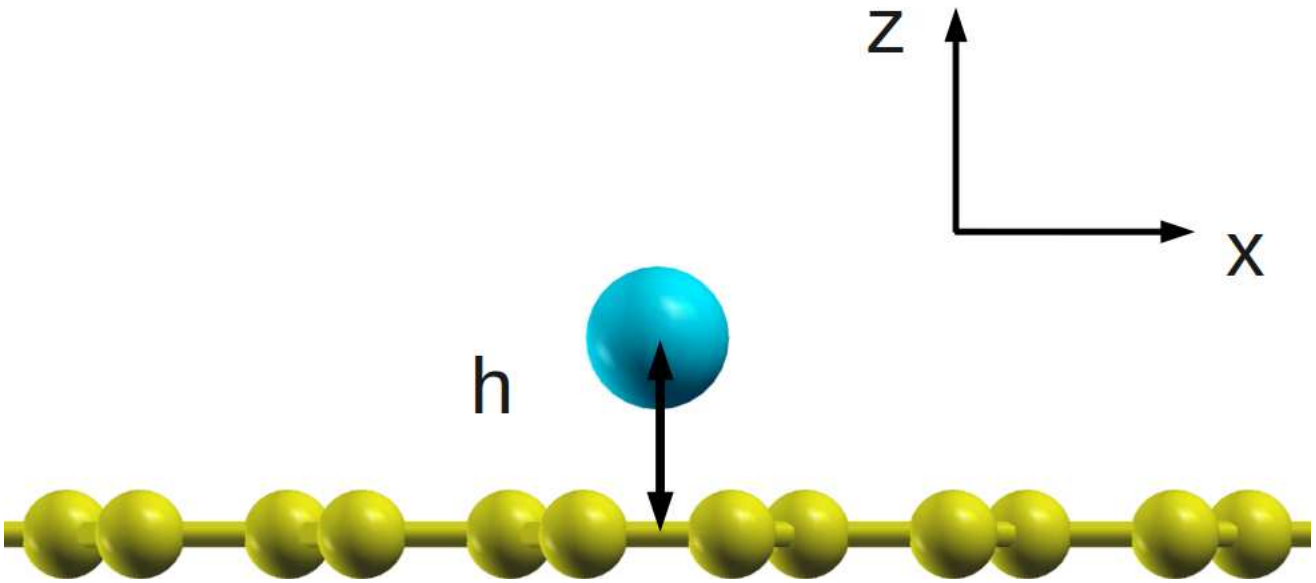

Figure 2 BX11058 13Dec2010

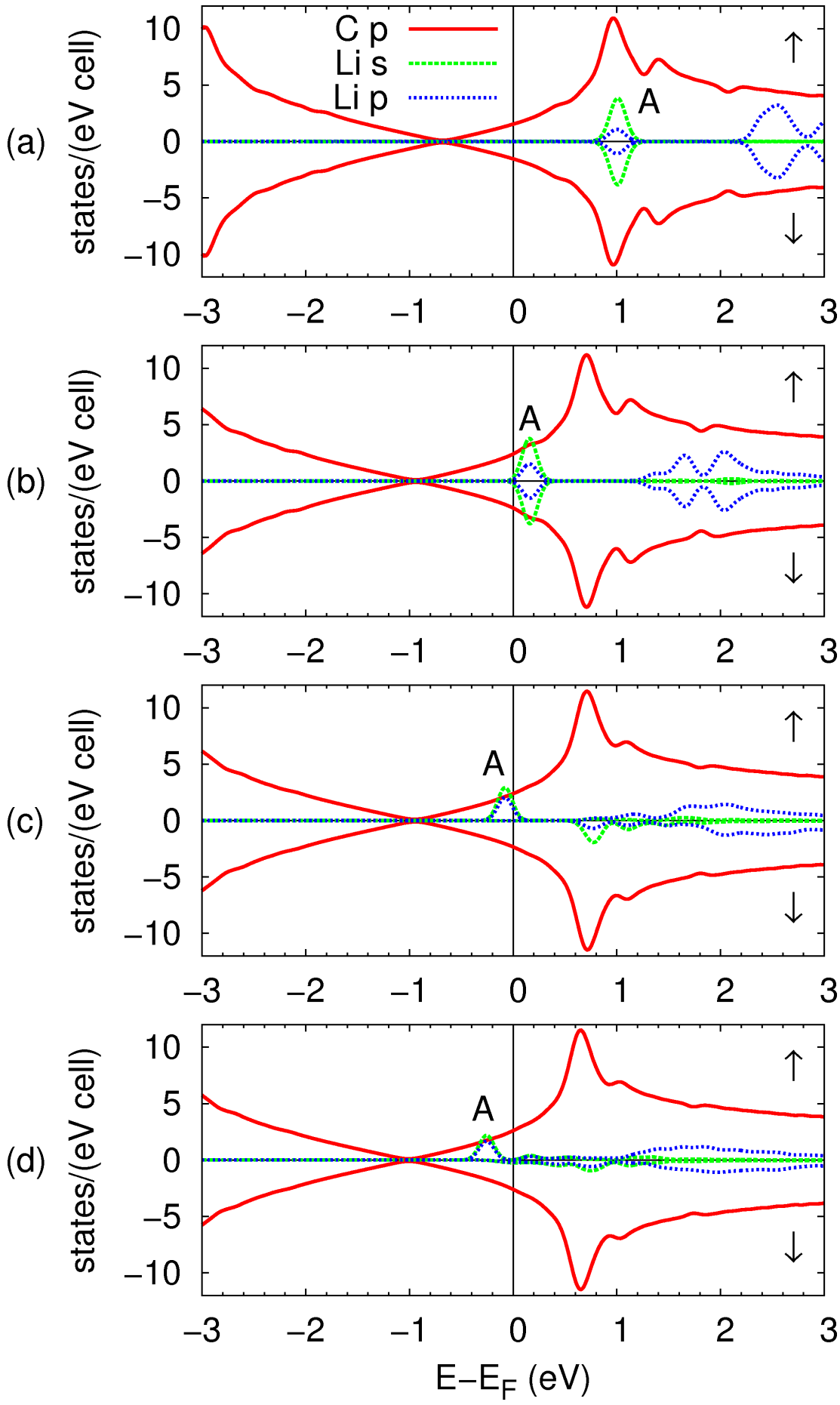

Figure 3 BX11058 13Dec2010

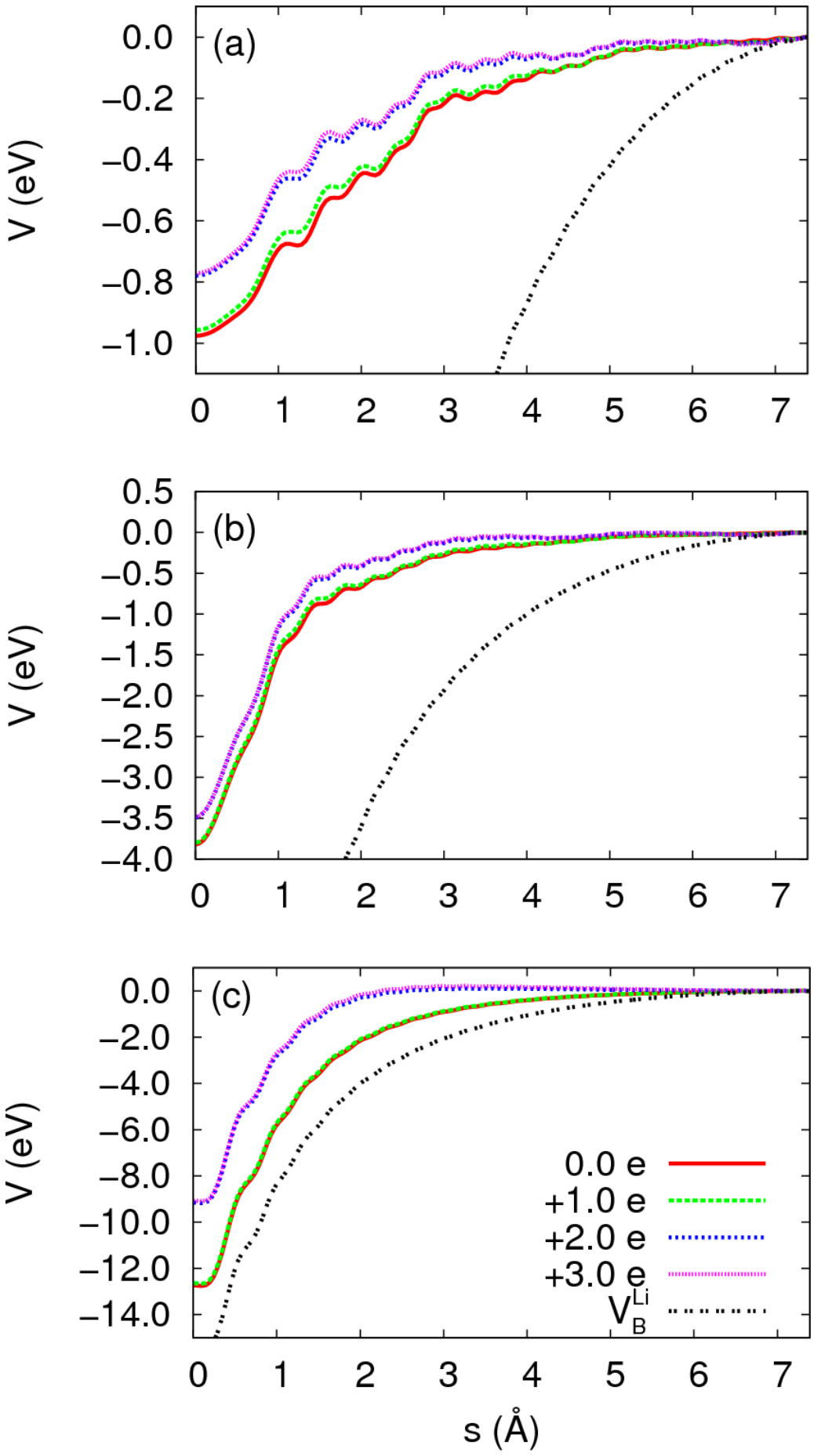

Figure 4 BX11058 13Dec2010

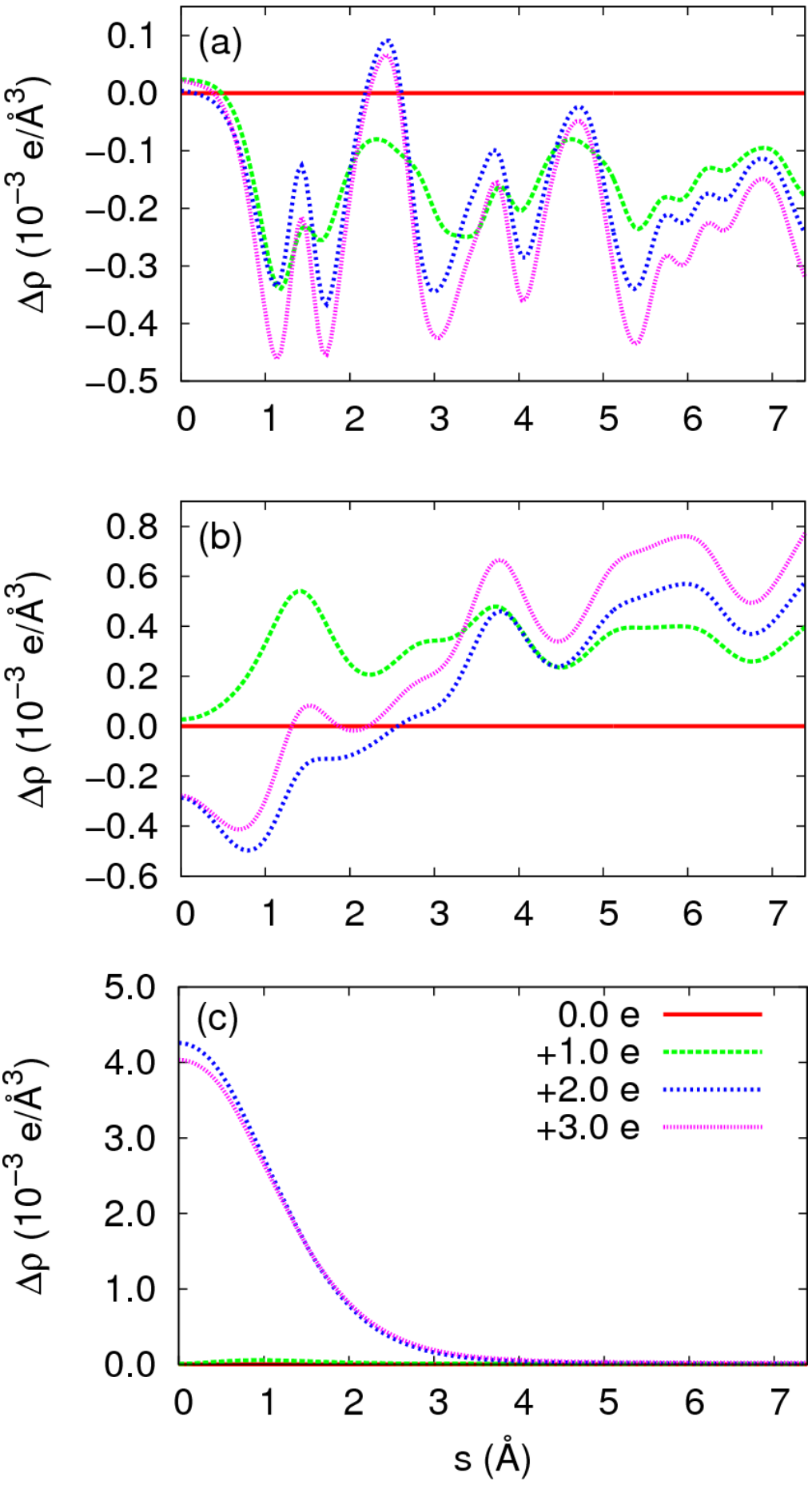

Figure 5 BX11058 13Dec2010

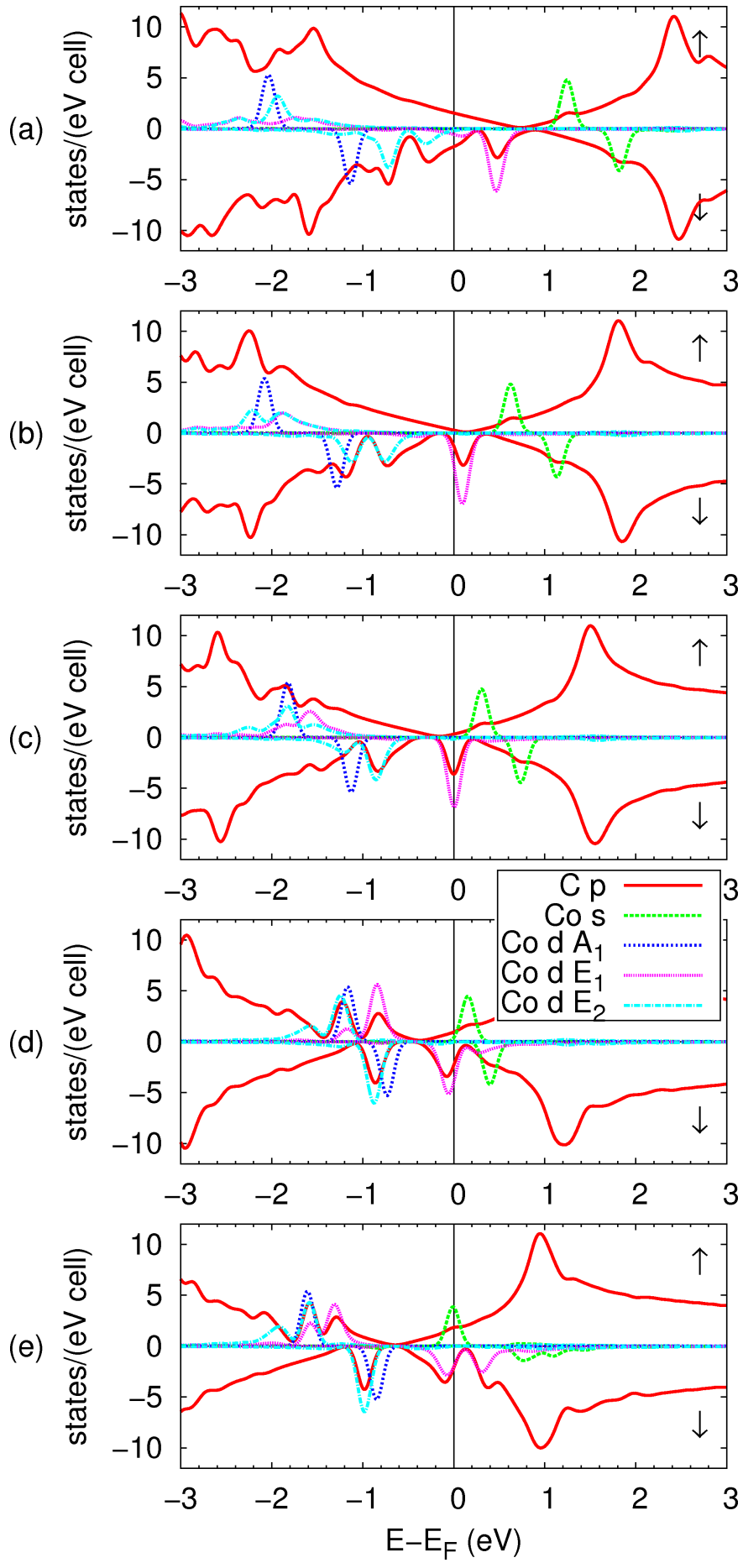

Figure 6 BX11058 13Dec2010

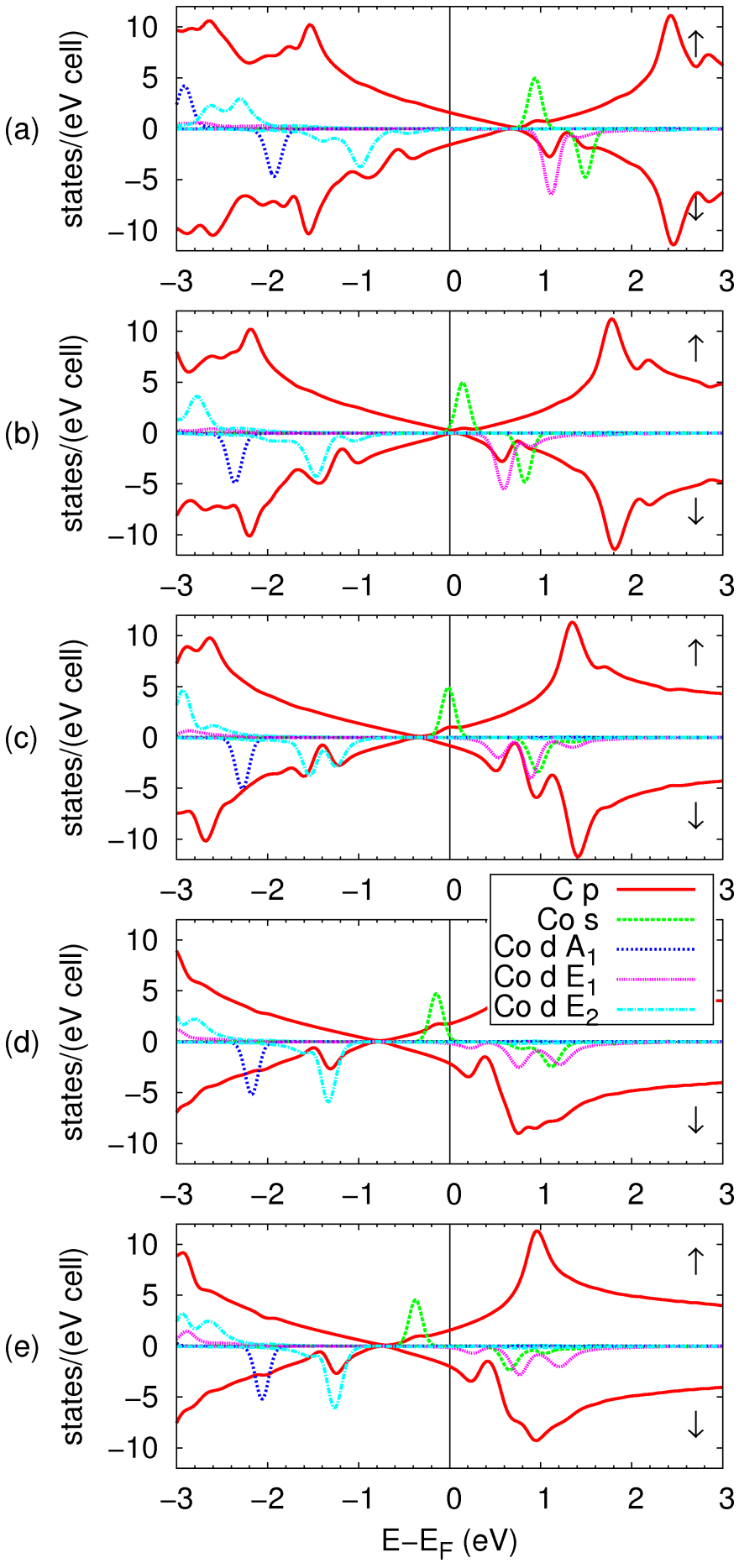

Figure 7 BX11058 13Dec2010

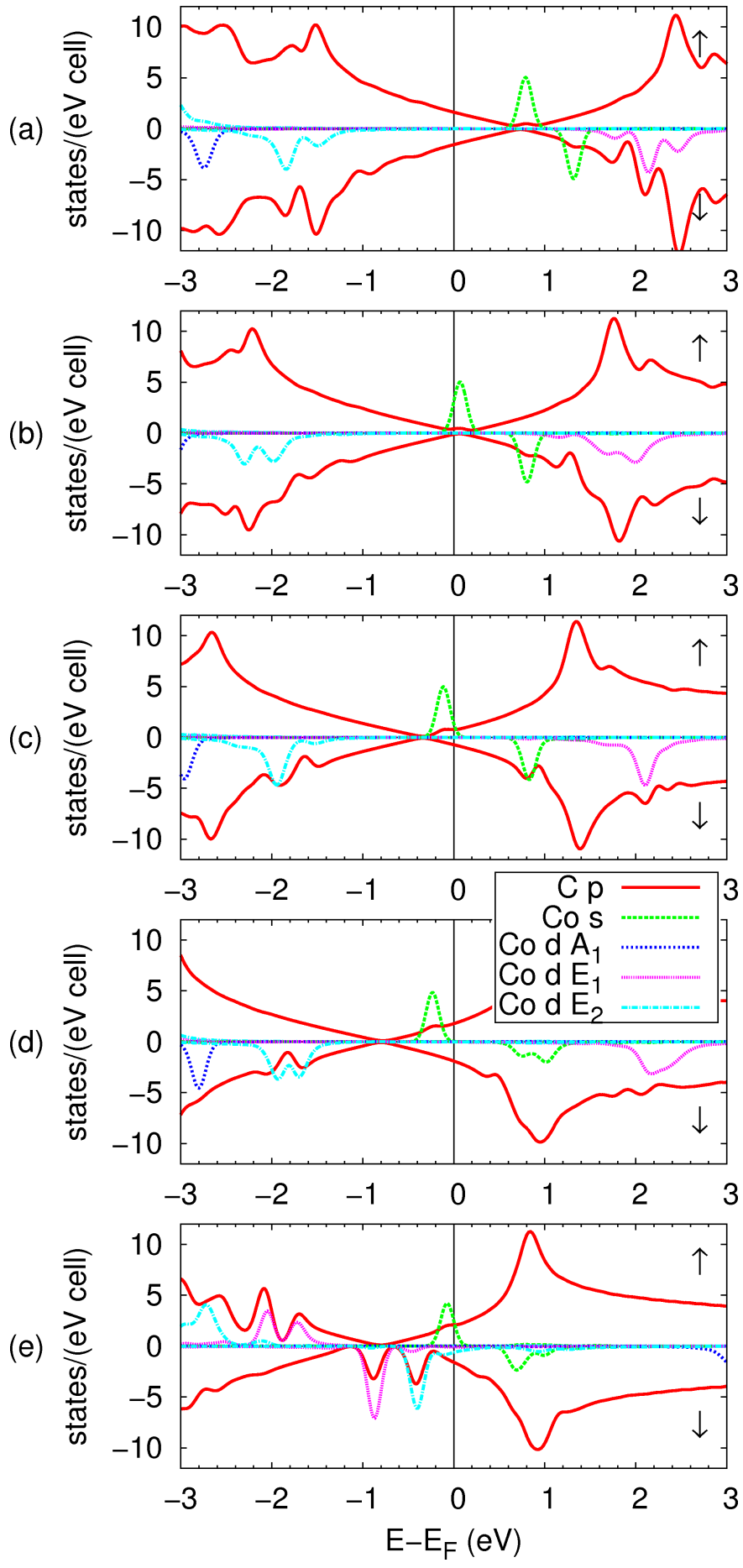

Figure 8 BX11058 13Dec2010

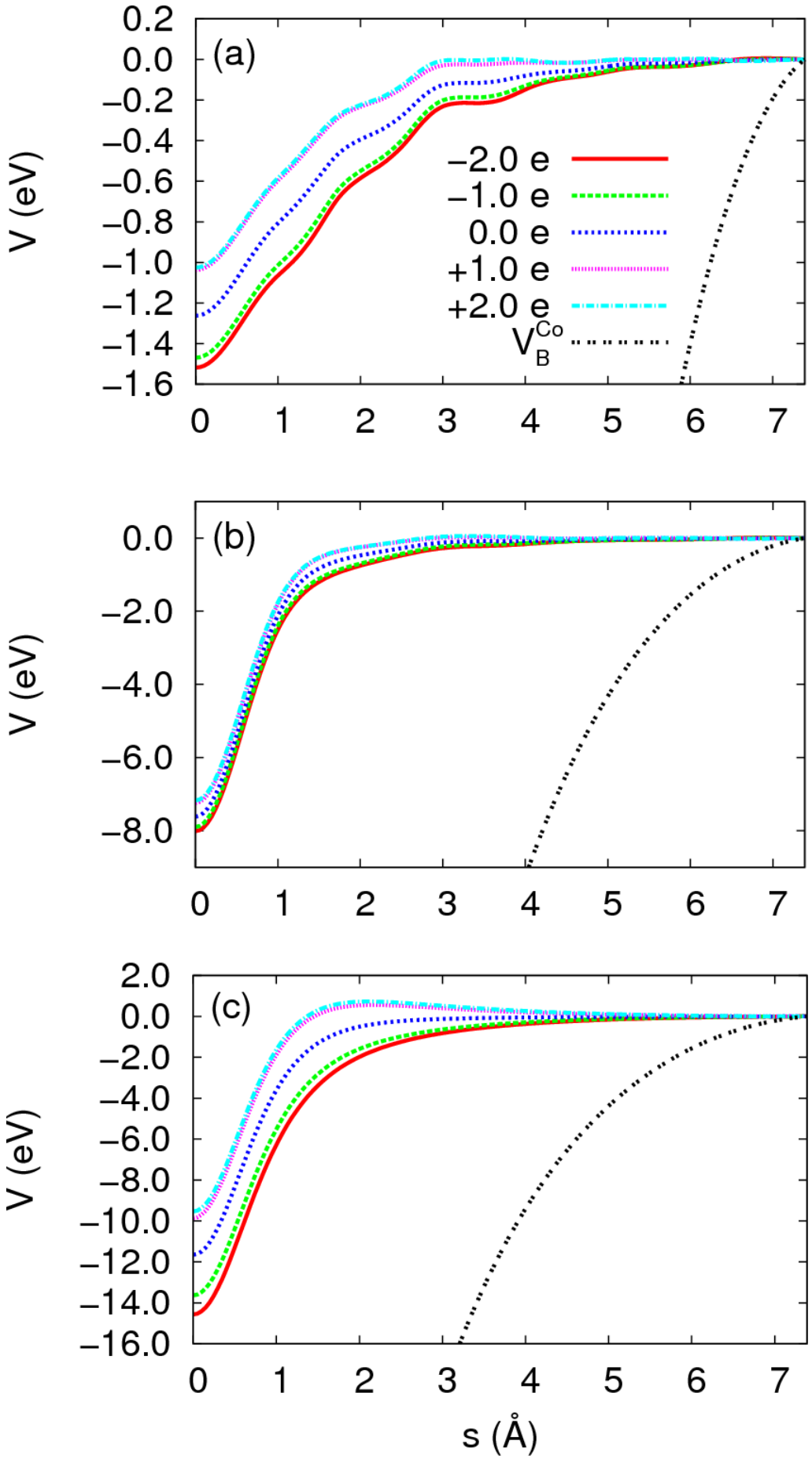

Figure 9 BX11058 13Dec2010

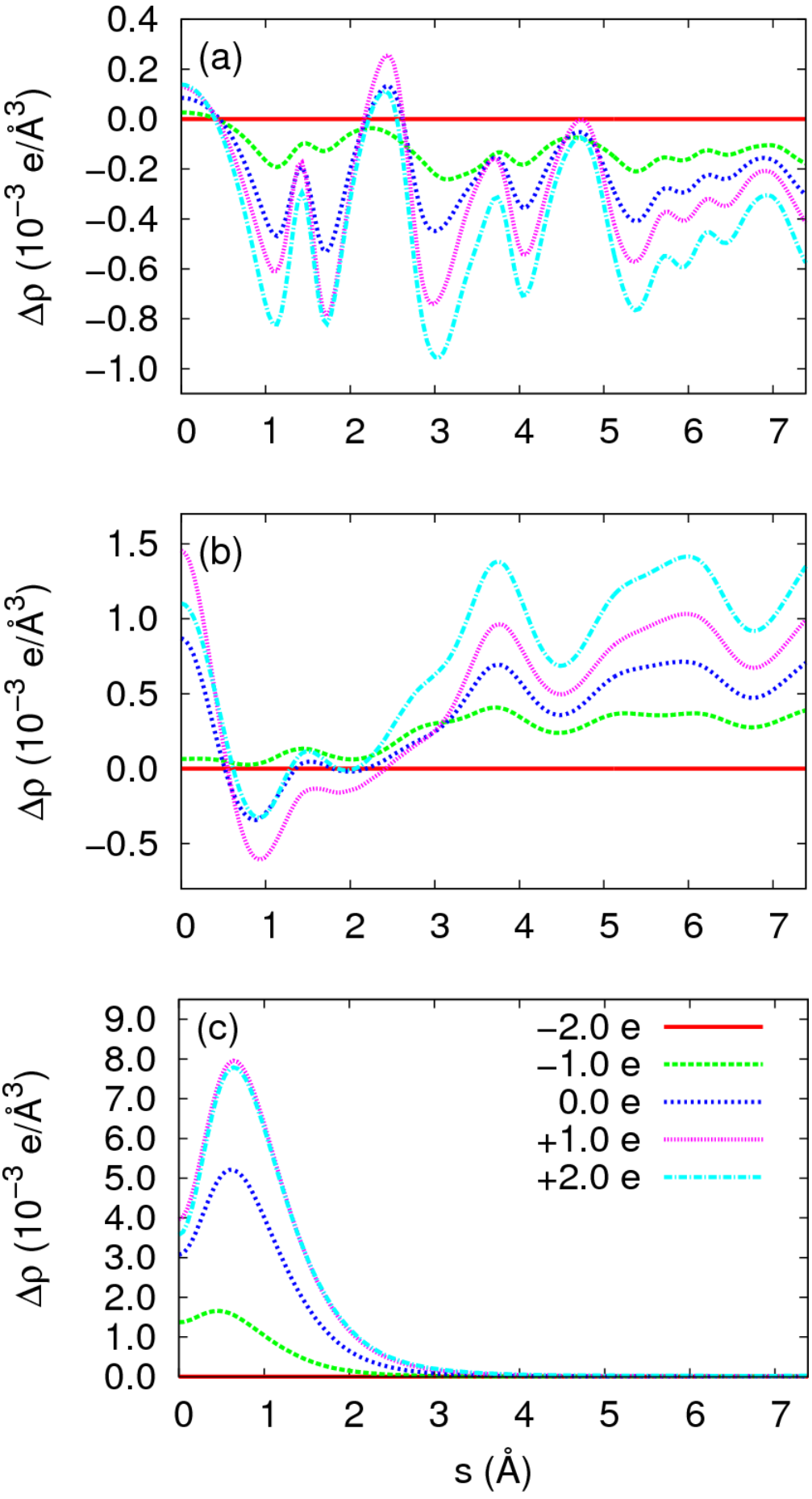

Figure 10 BX11058 13Dec2010